NASA Technical Memorandum 83200

STRESS-INTENSITY FACTOR EQUATIONS FOR CRACKS IN THREE-DIMENSIONAL FINITE BODIES

J. C. Newman, Jr. and I. S. Raju

August 1981

National Aeronautics and Space Administration

Langley Research Center
Hampton, Virginia 23665

STRESS-INTENSITY FACTOR EQUATIONS FOR CRACKS IN THREE-DIMENSIONAL FINITE BODIES

J. C. Newman, Jr.[1] and I. S. Raju[2]

NASA Langley Research Center

Hampton, Virginia 23665

SUMMARY

This paper presents empirical stress-intensity factor equations for embedded elliptical cracks, semi-elliptical surface cracks, quarter-elliptical corner cracks, semi-elliptical surface cracks at a hole, and quarter-elliptical corner cracks at a hole in finite plates. The plates were subjected to remote tensile loading. These equations give stress-intensity factors as a function of parametric angle, crack depth, crack length, plate thickness, and, where applicable, hole radius. The stress-intensity factors used to develop the equations were obtained from current and previous three-dimensional finite-element analyses of these crack configurations. A wide range of configuration parameters was included in the equations. The ratio of crack depth to plate thickness ranged from 0 to 1, the ratio of crack depth to crack length ranged from 0.2 to 2, and the ratio of hole radius to plate thickness ranged from 0.5 to 2. The effects of plate width on stress-intensity variations along the crack front were also included, but were generally based on engineering estimates. For all combinations of parameters investigated, the empirical

---

[1]Research Engineer, NASA Langley Research Center, Hampton, VA 23665

[2]Assistant Research Professor, The George Washington University, Joint Institute for Advancement of Flight Sciences, NASA Langley Research Center, Hampton, VA 23665

equations were generally within 5 percent of the finite-element results, except within a thin "boundary layer" where the crack front intersects a free surface. However, the proposed equations are expected to give a good estimate in this region because of a study made on the boundary-layer effect.

These equations should be useful for correlating and predicting fatigue-crack-growth rates as well as in computing fracture toughness and fracture loads for these types of crack configurations.

INTRODUCTION

In aircraft structures, fatigue failures usually occur from the initiation and propagation of cracks from notches or defects in the material that are either embedded, on the surface, or at a corner. These cracks propagate with elliptic or near-elliptic crack fronts. To predict crack-propagation life and fracture strength, accurate stress-intensity factor solutions are needed for these crack configurations. But, because of the complexities of such problems, exact solutions are not available. Instead, investigators have used approximate analytical methods, experimental methods, or engineering estimates to obtain the stress-intensity factors.

Very few exact solutions for three-dimensional cracked bodies are available in the literature. One of these, an elliptical crack in an infinite solid subjected to uniform tension, was derived by Irwin [1] using an exact stress analysis by Green and Sneddon [2]. For finite bodies, all solutions have required approximate analytical methods. For a semi-circular surface crack in a semi-infinite solid and a semi-elliptical surface crack in a plate of finite thickness, Smith, Emery, and Kobayashi [3], and Kobayashi [4], respectively, used the alternating method to obtain stress-intensity factors along the crack front. Raju and Newman [5,6] used the finite-element method, and Heliot, Labbens, and Pellissier-Tanon [7] used the boundary-integral equation method to obtain the same information. For a quarter-elliptic corner crack in a plate, Tracey [8] and Pickard [9] used the finite-element method; Kobayashi and Enetanya [10] used the alternating method. Shah [11] estimated the stress-intensity factors for a surface crack emanating from a circular hole. For a single corner crack emanating from a circular hole in a plate, Smith and Kullgren [12] used a finite-element-alternating method to obtain the stress-

intensity factors. Hechmer and Bloom [13] and Raju and Newman [14] used the finite-element method for two-symmetric corner cracks emanating from a hole in a plate. All of these approximate results, except that for the surface crack [6,9] and the corner crack [9], were presented in the form of curves or tables. However, for ease of computation, results expressed in the form of equations are preferable.

The present paper presents empirical equations for the stress-intensity factors for a wide variety of three-dimensional crack configurations subjected to uniform tension as a function of parametric angle, crack depth, crack length, plate thickness, and hole radius (where applicable), for example see Figure 1. These crack configurations, shown in Figure 2, include: an embedded elliptical crack, a semi-elliptical surface crack, a quarter-elliptical corner crack, a semi-elliptical surface crack at a hole, and a quarter-elliptical corner crack at a hole in finite plates subjected to remote tensile loading. The equations were based on the stress-intensity factors obtained from three-dimensional finite-element analyses conducted herein and from the literature [5,14], and cover a wide range of configuration parameters. The ratio of crack depth to plate thickness (a/t) ranged from 0 to 1, the ratio of crack depth to crack length (a/c) ranged from 0.2 to 2, and the ratio of hole radius to plate thickness (R/t) ranged from 0.5 to 2. The effects of plate width (b) on stress-intensity variations along the crack front were also included, but were generally based on engineering estimates.

SYMBOLS

a	depth of crack
b	width or half-width of cracked plate (see Fig. 2)
c	length or half-length of crack (see Fig. 2)
F	boundary-correction factor on stress intensity
F_c	boundary-correction factor for corner crack in a plate
F_e	boundary-correction factor for embedded crack in a plate
F_s	boundary-correction factor for surface crack in a plate
F_{sh}	boundary-correction factor for surface crack at a hole in a plate
F_{ch}	boundary-correction factor for corner crack at a hole in a plate
f_w	finite-width correction factor
f_ϕ	angular function derived from embedded elliptical crack solution
g_i	curve fitting functions defined in text
h	half-length of cracked plate
K_I	stress-intensity factor (Mode I)
M_i	curve fitting functions defined in text
Q	shape factor for an elliptical crack
R	radius of hole
S	remote uniform tensile stress
t	thickness or half-thickness of plate (see Fig. 2)
ν	Poisson's ratio
ϕ	parametric angle of the ellipse

THREE-DIMENSIONAL FINITE-ELEMENT ANALYSES

Three-dimensional finite-element analyses [5,14] using linear-strain and singularity elements were used herein to calculate the mode I stress-intensity factor variation along the crack front for an embedded elliptical crack, a quarter-elliptical corner crack, and a semi-elliptical surface crack at a hole in a finite plate subjected to remote tensile loading (see Fig. 2). The finite-element models used for these configurations were the same as those used in references 5 and 14 for surface cracks and corner cracks at holes. The only differences were the boundary conditions that were imposed on certain faces of the models. For embedded cracks and surface cracks at holes, the normal displacements on three planes of symmetry were fixed (set equal to zero), except for the crack surface. For a corner crack in a plate, the normal displacements on the two faces that intersect the crack were free.

The stress-intensity factors were obtained from the finite-element analyses by using a nodal-force method, the details of which are given in references 5 and 15. In this method, the nodal forces normal to the crack plane and ahead of the crack front were used to evaluate the stress-intensity factors.

The stress-intensity factor, K_I, at any point along the crack front in a finite-thickness plate was taken to be

$$K_I = S\sqrt{\pi\frac{a}{Q}}\,F\left(\frac{a}{t}, \frac{a}{c}, \frac{R}{t}, \phi\right) \qquad (1)$$

where Q is the shape factor for an ellipse and is given by the square of the complete elliptic integral of the second kind [2]. In the finite-element models, the width (b) and length (h) of the plate were taken to be large enough

so that they would have a negligible effect on stress intensity. The boundary correction, F, accounts for the influence of various boundaries and is a function of crack depth, crack length, hole radius (where applicable), plate thickness, and the parametric angle of the ellipse. Figure 3 shows the coordinate system used to define the parametric angle.

Very useful empirical expressions for Q have been developed by Rawe (see ref. 6). The expressions are

$$Q = 1 + 1.464\left(\frac{a}{c}\right)^{1.65} \quad \text{for } \frac{a}{c} \leq 1 \tag{2a}$$

$$Q = 1 + 1.464\left(\frac{c}{a}\right)^{1.65} \quad \text{for } \frac{a}{c} > 1 \tag{2b}$$

The maximum error in the stress-intensity factor by using these equations for Q was about 0.13 percent for all values of a/c. (Rawe's original equation was written in terms of a/2c).

The boundary-correction factors, F, obtained from the present finite-element results for the embedded elliptical crack and the quarter-elliptic corner crack in a finite plate subjected to uniform tension are given in Tables 1 and 2, respectively, for various parametric angles and several a/c and a/t ratios. Tables 3a and 3b give the boundary-correction factors for two-symmetric semi-elliptical surface cracks emanating from a circular hole in a finite plate subjected to uniform tension for R/t equal 1 and 2, respectively.

STRESS-INTENSITY FACTOR EQUATIONS

In the following sections, the empirical stress-intensity factor equations for embedded elliptical cracks, semi-elliptical surface cracks, quarter-elliptical corner cracks, semi-elliptical surface cracks at a hole, and quarter-elliptical corner cracks at a hole in finite plates (see Figure 2) subjected to remote tension are presented. The particular functions chosen were obtained from systematic curve-fitting procedure by using double-series polynomials in terms of a/c, a/t, and angular functions of ϕ. For cracks emanating from holes, polynomial equations in terms of c/R and ϕ were also used.

Embedded Elliptical Crack

The empirical stress-intensity factor equation for an embedded elliptical crack in a finite plate, Figure 2a, subjected to tension was obtained by fitting to the finite-element results presented herein (Table 1). To account for limiting behavior as a/c approaches zero or infinity, the results of Irwin [1] were also used. The equation is

$$K_I = S\sqrt{\pi\frac{a}{Q}}\, F_e\left(\frac{a}{c}, \frac{a}{t}, \frac{c}{b}, \phi\right) \tag{3}$$

for $0 \le a/c \le \infty$, $c/b < 0.5$, and $-\pi \le \phi \le \pi$ provided that a/t satisfies:

$$\left.\begin{aligned} \frac{a}{t} &< 1.25\left(\frac{a}{c} + 0.6\right) && \text{for } 0 \le \frac{a}{c} \le 0.2 \\ \frac{a}{t} &< 1 && \text{for } 0.2 \le \frac{a}{c} \le \infty \end{aligned}\right\} \tag{4}$$

The function F_e accounts for the influence of crack shape (a/c), crack size (a/t), finite width (c/b), and angular location (ϕ), and was chosen as

$$F_e = \left[M_1 + M_2 \left(\frac{a}{t}\right)^2 + M_3 \left(\frac{a}{t}\right)^4\right] g\, f_\phi\, f_w \tag{5}$$

The term in brackets gives the boundary-correction factors at $\phi = \pi/2$ (where $g = f_\phi = 1$). The function f_ϕ was taken from the exact solution for an embedded elliptical crack in an infinite solid [1] and f_w is a finite-width correction factor. The function g is a fine-tuning curve-fitting function. For $a/c \leq 1$:

$$M_1 = 1 \tag{6}$$

$$M_2 = \frac{0.05}{0.11 + \left(\frac{a}{c}\right)^{3/2}} \tag{7}$$

$$M_3 = \frac{0.29}{0.23 + \left(\frac{a}{c}\right)^{3/2}} \tag{8}$$

$$g = 1 - \frac{\left(\frac{a}{t}\right)^4}{1 + 4\left(\frac{a}{c}\right)} \cos\phi \tag{9}$$

and

$$f_\phi = \left[\left(\frac{a}{c}\right)^2 \cos^2\phi + \sin^2\phi\right]^{1/4} \tag{10}$$

The finite-width correction, f_w, from Reference 6 was

$$f_w = \left[\sec\left(\frac{\pi c}{2b}\sqrt{\frac{a}{t}}\right)\right]^{1/2} \tag{11}$$

for $c/b < 0.5$. (Note that for the embedded crack, t is defined as one-half of the full plate thickness.) For $a/c > 1$:

$$M_1 = \sqrt{\frac{c}{a}} \tag{12}$$

and

$$f_\phi = \left[\left(\frac{c}{a}\right)^2 \sin^2\phi + \cos^2\phi\right]^{1/4} \tag{13}$$

The functions M_2, M_3, g, and f_w are given by equations (7), (8), (9), and (11), respectively.

As a/c approaches zero and ϕ equals $\pi/2$, the stress-intensity factor equation reduces to

$$K_I = S\sqrt{\pi a}\left[1 + 0.455\left(\frac{a}{t}\right)^2 + 1.261\left(\frac{a}{t}\right)^4\right] \tag{14}$$

for $c/b = 0$.

Equation (14) is within 1 percent of the accepted solution [16] for $a/t < 0.55$ and within 3 percent for $a/t < 0.8$.

As a/c approaches infinity and ϕ equals zero, the equation reduces to

$$K_I = S\sqrt{\pi c}\left[\sec\left(\frac{\pi c}{2b}\sqrt{\frac{a}{t}}\right)\right]^{1/2} \qquad (15)$$

Equation (15) is the accepted solution [16] for this configuration as a/t approaches unity.

A typical comparison between the proposed equation and the finite-element results for an embedded elliptical crack is shown in Figure 4 for $a/c = 0.4$ and various a/t ratios. The boundary-correction factor, F_e, is plotted against the parametric angle. At $\phi = 0$ and $\pi/2$, the equation (solid curves) is within 2 percent of the finite-element results (symbols). (Herein "percent error" is defined as the difference between the equation and the finite-element results normalized by the maximum value for that particular case. This definition is necessary because the stress-intensity factors in some cases vary from small to large values along the crack front.) The dashed curve shows the exact solution for an elliptic crack in an infinite solid [1]. These results indicate that the finite-element solution for $a/t = 0.2$ is probably about 1.5 percent below the exact solution. Because the proposed equation is slightly higher than the finite-element results, the equation should be very accurate.

Semi-elliptical Surface Crack

An empirical equation for the stress-intensity factors for a semi-elliptical surface crack in a finite plate, Figure 2b, subjected to tension was obtained from Reference 6. This equation was previously fitted to the finite-element results from Raju and Newman [5] for a/c values from 0.2 to 1. An

equation for a/c greater than unity was developed herein. To account for the limiting behavior as a/c approaches zero, the results of Gross and Srawley [17] for a single-edge crack were also used. The equation is

$$K_I = S\sqrt{\pi\frac{a}{Q}}\,F_s\left(\frac{a}{c}, \frac{a}{t}, \frac{c}{b}, \phi\right) \tag{16}$$

for $0 \leq a/c \leq 2$, $c/b < 0.5$, and $0 \leq \phi \leq \pi$, again, provided that a/t satisfies equations (4). The function F_s was chosen to be

$$F_s = \left[M_1 + M_2\left(\frac{a}{t}\right)^2 + M_3\left(\frac{a}{t}\right)^4\right] g\, f_\phi\, f_w \tag{17}$$

For $a/c \leq 1$:

$$M_1 = 1.13 - 0.09\left(\frac{a}{c}\right) \tag{18}$$

$$M_2 = -0.54 + \frac{0.89}{0.2 + \left(\frac{a}{c}\right)} \tag{19}$$

$$M_3 = 0.5 - \frac{1}{0.65 + \frac{a}{c}} + 14\left(1 - \frac{a}{c}\right)^{24} \tag{20}$$

$$g = 1 + \left[0.1 + 0.35\left(\frac{a}{t}\right)^2\right](1 - \sin\phi)^2 \tag{21}$$

and f_ϕ is given by equation (10). The finite-width correction, f_w, is again, given by equation (11). Equations (17) through (21) were taken from Reference 6.

For $a/c > 1$:

$$M_1 = \sqrt{\frac{c}{a}}\left(1 + 0.04 \ \frac{c}{a}\right) \tag{22}$$

$$M_2 = 0.2\left(\frac{c}{a}\right)^4 \tag{23}$$

$$M_3 = -0.11\left(\frac{c}{a}\right)^4 \tag{24}$$

$$g = 1 + \left[0.1 + 0.35\left(\frac{c}{a}\right)\left(\frac{a}{t}\right)^2\right](1 - \sin\phi)^2 \tag{25}$$

and f_ϕ and f_w are given by equations (13) and (11), respectively.

Figure 5 shows the distribution of boundary-correction factors, F_s, along the crack front for a semi-elliptical surface crack with $a/c = 2$ for two a/t ratios. The proposed equation (solid curves) is within 3 percent of the finite-element results (symbols).

For $a/c \leq 1$, Reference 6 gives a more complete comparison between the proposed equation and the finite-element results. In Reference 6, the equation was also used to predict surface-crack-growth patterns under tension fatigue loads. These predicted crack-growth patterns were in good agreement with measurements made on steel, titanium alloy, and aluminum alloy materials. In Reference 18, the equation was also used to correlate surface-crack fracture data for a brittle epoxy material within ± 10 percent over a wide range of crack shapes (a/c) and crack sizes (a/t).

Quarter-elliptical Corner Crack

The empirical stress-intensity factor equation for a quarter-elliptical corner crack in a finite plate, Figure 2c, subjected to tension was obtained by fitting to the finite-element results presented herein (Table 2). The equation is

$$K_I = S\sqrt{\pi\frac{a}{Q}}\ F_c\left(\frac{a}{c}, \frac{a}{t}, \phi\right) \tag{26}$$

for $0.2 \leq a/c \leq 2$, $a/t < 1$, and $0 \leq \phi \leq \pi/2$ for $c/b < 0.2$. The function F_c was chosen as

$$F_c = \left[M_1 + M_2\left(\frac{a}{t}\right)^2 + M_3\left(\frac{a}{t}\right)^4\right] g_1\ g_2\ f_\phi \tag{27}$$

(Although the effects of width are significant, f_w is not included in equation (27) because results on finite-width plates were not available for comparison.) For $a/c \leq 1$:

$$M_1 = 1.08 - 0.03\left(\frac{a}{c}\right) \tag{28}$$

$$M_2 = -0.44 + \frac{1.06}{0.3 + \left(\frac{a}{c}\right)} \tag{29}$$

$$M_3 = -0.5 + 0.25\left(\frac{a}{c}\right) + 14.8\left(1 - \frac{a}{c}\right)^{15} \tag{30}$$

$$g_1 = 1 + \left[0.08 + 0.4\left(\frac{a}{t}\right)^2\right](1 - \sin\phi)^3 \tag{31}$$

$$g_2 = 1 + \left[0.08 + 0.15\left(\frac{a}{t}\right)^2\right](1 - \cos\phi)^3 \qquad (32)$$

and f_ϕ is given by equation (10).

For $a/c > 1$:

$$M_1 = \sqrt{\frac{c}{a}}\left(1.08 - 0.03\,\frac{c}{a}\right) \qquad (33)$$

$$M_2 = 0.375\left(\frac{c}{a}\right)^2 \qquad (34)$$

$$M_3 = -0.25\left(\frac{c}{a}\right)^2 \qquad (35)$$

$$g_1 = 1 + \left[0.08 + 0.4\left(\frac{c}{t}\right)^2\right](1 - \sin\phi)^3 \qquad (36)$$

$$g_2 = 1 + \left[0.08 + 0.15\left(\frac{c}{t}\right)^2\right](1 - \cos\phi)^3 \qquad (37)$$

and f_ϕ is given by equation (13).

Figure 6 shows boundary-correction factors obtained by several investigators for a quarter-circular corner crack in a finite-thickness plate ($a/t = 0.2$) under tension loading. The present finite-element results are shown as solid circular symbols and the proposed equation is shown as the solid curve. Tracey [8] and Pickard [9] also used the finite-element method, but the width (b) and half-length (h) of their models were equal to the plate thickness (see

dashed and dash-dot lines in the insert). Kobayashi [10] used the alternating method, but the a/c ratio was 0.98. Pickard's results were 1 to 3 percent higher than the present finite-element results. Part of the difference is due to a width- and length-effect in Pickard's model. And the present results are expected to be about 1.5 percent below the exact solution. Near $\phi = 0$ and $\pi/2$, Tracey's and Kobayashi's results are 5 to 13 percent higher than the present results. All results are in good agreement (within 3 percent) at the mid-point ($\phi = \pi/4$).

Figures 7 and 8 show the distribution of boundary-correction factors, F_c, along the crack front for a quarter-circular (a/c = 1) and semi-elliptical (a/c = 0.2) corner crack, respectively, in a finite plate subjected to tension. The figures show the results for several a/t ratios. The proposed equation (solid curves) is generally within about 2 percent of the finite-element results (symbols), except near the intersection of the crack front with the free surfaces ($\phi = 0$ and $\pi/2$). Near these points, the equation is generally higher than the finite-element results. The maximum difference being about 5 percent. These low values at the free surfaces are probably due to a boundary-layer effect [19] and this behavior is discussed in the appendix.

Semi-elliptical Surface Crack at Hole

Two-symmetric surface cracks.- The empirical stress-intensity factor equation for two-symmetric semi-elliptical surface cracks at the center of a hole in a finite plate, Figure 2d, subjected to tension was obtained by fitting to the finite-element results presented here (Tables 3a and 3b). The equation is

$$K_I = S\sqrt{\pi\frac{a}{Q}}\ F_{sh}\left(\frac{a}{c}, \frac{a}{t}, \frac{R}{t}, \frac{R}{b}, \frac{c}{b}, \phi\right) \tag{38}$$

for $0.2 \leq a/c \leq 2$, $a/t < 1$, $0.5 \leq R/t \leq 2$, $(R + c)/b < 0.5$, and $-\pi/2 \leq \phi \leq \pi/2$. (Note that here t is defined as one-half of the full plate thickness.) The function F_{sh} was chosen as

$$F_{sh} = \left[M_1 + M_2\left(\frac{a}{t}\right)^2 + M_3\left(\frac{a}{t}\right)^4\right] g_1\ g_2\ f_\phi\ f_w \tag{39}$$

For $a/c \leq 1$:

$$M_1 = 1 \tag{40}$$

$$M_2 = \frac{0.05}{0.11 + \left(\frac{a}{c}\right)^{3/2}} \tag{41}$$

$$M_3 = \frac{0.29}{0.23 + \frac{a}{c}^{3/2}} \tag{42}$$

$$g_1 = 1 - \frac{\left(\frac{a}{t}\right)^4}{1 + 4\left(\frac{a}{c}\right)}\cos\phi \tag{43}$$

$$g_2 = \frac{1 - 0.15\lambda + 3.46\lambda^2 - 4.47\lambda^3 + 3.52\lambda^4}{1 + 0.08\lambda^2} \tag{44}$$

where

$$\lambda = \frac{1}{1 + \frac{c}{R} \cos\ (0.9\ \phi)} \tag{45}$$

The function f_ϕ is given by equation (10). The finite-width correction, f_w, was taken as

$$f_w = \left[\sec\left(\frac{\pi R}{2b}\right) \sec\left(\frac{\pi(2R+nc)}{4(b-c) + 2nc} \sqrt{\frac{a}{t}}\right)\right]^{1/2} \tag{46}$$

where $n = 1$ is for a single crack and $n = 2$ is for two-symmetric cracks. This equation was chosen to account for the effects of width on stress concentration at the hole [20] and for crack eccentricity [16]. For $a/c > 1$:

$$M_1 = \sqrt{\frac{c}{a}} \tag{47}$$

The functions M_2, M_3, g_1, g_2, and λ are given by equations (41) through (45), and the functions f_ϕ and f_w are given by equation (13) and (46), respectively.

Estimates for a single-surface crack.- The stress-intensity factors for a single-surface crack located at the center of a hole can be estimated from the present results for two-symmetric surface cracks by using a conversion factor developed by Shah [11]. The relationship between one- and two-surface cracks was given by

$$(K_I)_{\substack{\text{one}\\\text{crack}}} = \sqrt{\frac{\frac{4}{\pi} + \frac{ac}{2tR}}{\frac{4}{\pi} + \frac{ac}{tR}}} \; (K_I)_{\substack{\text{two}\\\text{cracks}}} \tag{48}$$

Shah had assumed that the conversion factor was constant for all locations along the crack front; that is, independent of the parametric angle.

Comparison with another stress-intensity solution.- Figure 9 shows a comparison between the present results and those estimated by Shah [11] for two-symmetric semi-circular (a/c = 1) and semi-elliptical (a/c = 0.2) surface cracks emanating from a hole in a plate subjected to tension. The present results (solid symbols) show the distribution of boundary-correction factors, F_{sh}, as a function of the parametric angle. The open symbols show the results estimated by Shah. The proposed equation (solid curves) is in good agreement with the results estimated by Shah, but the equation is about 5 percent higher (based on peak value) than the present results in the mid-region for the semi-elliptic crack. Near the intersection of the crack front with the free surface ($\phi = \pi/2$), the present results show a sharp reduction. As previously mentioned, this reduction is probably due to a boundary-layer effect (see Appendix). However, as mentioned in the Appendix, further mesh refinement in this region causes the stress-intensity factors to be higher very near the intersection point, but lower at the surface. Also, the stress-intensity factors in the interior region $0 \leq 2\phi/\pi < 0.8$ were unaffected by mesh refinement. Therefore, the equation was fitted in the interior region ($2\phi/\pi < 0.8$) only. However, the proposed equation, extrapolated to the surface, is probably a good estimate for the limiting behavior due to mesh refinement.

The influence of crack shape (a/c) on the distribution of boundary-correction factors is shown in Figure 10. The open symbols show the estimated results from Shah [11]. And the solid symbols show the present finite-element results for a/c = 2. The solid curves show the results from the proposed equation for a semi-elliptical surface crack at a hole with R/t = 0.5. The agreements are very good.

Effects of crack depth-to-plate thickness.- Figure 11 shows the distribution of boundary-correction factors, F_{sh}, along the crack fron for two-symmetric semi-circular surfacr cracks at a hole (R/t = 1) with various a/t ratios. The proposed equation (solid curves) is generally within a few percent of the finite-element results (symbols), except near the intersection of the crack front with the hole surface ($\phi = \pi/2$). Here, again, the proposed equation is expected to give a good estimate for the limiting behavior due to mesh refinement in this region.

Quarter-elliptical Corner Crack at a Hole

Two-symmetric corner cracks.- The empirical stress-intensity factor equation for two-symmetric quarter-elliptical corner cracks at a hole in a finite plate, Figure 2e, subjected to tension was obtained by fitting to the finite-element results in Reference 14. The equation is

$$K_I = S\sqrt{\pi\frac{a}{Q}}\ F_{ch}\left(\frac{a}{c}, \frac{a}{t}, \frac{R}{t}, \frac{R}{b}, \frac{c}{b}, \phi\right) \qquad (49)$$

for $0.2 \le a/c \le 2$, $a/t < 1$, $0.5 \le R/t \le 1$, $(R + c)/b < 0.5$, and $0 \le \phi \le \pi/2$. The function F_{ch} was chosen as

$$F_{ch} = \left[M_1 + M_2 \left(\frac{a}{t}\right)^2 + M_3 \left(\frac{a}{t}\right)^4 \right] g_1 g_2 g_3 f_\phi f_w \qquad (50)$$

For $a/c \leq 1$:

$$M_1 = 1.13 - 0.09 \left(\frac{a}{c}\right) \qquad (51)$$

$$M_2 = -0.54 + \frac{0.89}{0.2 + \frac{a}{c}} \qquad (52)$$

$$M_3 = 0.5 - \frac{1}{0.65 + \frac{a}{c}} + 14 \left(1 - \frac{a}{c}\right)^{24} \qquad (53)$$

$$g_1 = 1 + \left[0.1 + 0.35 \left(\frac{a}{t}\right)^2 \right] (1 - \sin \phi)^2 \qquad (54)$$

$$g_2 = \frac{1 - 0.15\lambda + 3.46\lambda^2 - 4.47\lambda^3 + 3.52\lambda^4}{1 + 0.13\lambda^2} \qquad (55)$$

where

$$\lambda = \frac{1}{1 + \frac{c}{R} \cos (0.85 \phi)} \qquad (56)$$

The function g_3 is given by

$$g_3 = \left(1 + 0.04 \frac{a}{c}\right) \left[1 + 0.1 (1 - \cos \phi)^2 \right] \left[0.8 + 0.2 \left(\frac{a}{t}\right)^{1/4} \right] \qquad (57)$$

Functions f_ϕ and f_w are given by equations (10) and (46), respectively.

For $a/c > 1$:

$$M_1 = \sqrt{\frac{c}{a}}\left(1 + 0.04\,\frac{c}{a}\right) \tag{58}$$

$$M_2 = 0.2\left(\frac{c}{a}\right)^4 \tag{59}$$

$$M_3 = -0.11\left(\frac{c}{a}\right)^4 \tag{60}$$

$$g_1 = 1 + \left[0.1 + 0.35\left(\frac{c}{a}\right)\left(\frac{a}{t}\right)^2\right](1 - \sin\phi)^2 \tag{61}$$

Functions g_2 and λ are given by equations (55) and (56). The function g_3 is given by

$$g_3 = \left(1.13 - 0.09\,\frac{c}{a}\right)\left[1 + 0.1\,(1 - \cos\phi)^2\right]\left[0.8 + 0.2\left(\frac{a}{t}\right)^{1/4}\right] \tag{62}$$

The functions f_ϕ and f_w are, again, given by equations (13) and (46), respectively.

Estimates for a single-corner crack.- The stress-intensity factors for a single-corner crack at a hole can be estimated from the present results for two-symmetric corner cracks by using the Shah-conversion factor (Eq. (48)). Raju and Newman [14] have evaluated the use of the conversion factor for some corner-crack-at-a-hole configurations. The stress-intensity factor obtained

using the conversion factor were in good agreement with the results from Smith and Kullgren [12] for a singl-corner crack at a hole.

Effects of plate thickness and crack shape.- Figures 12 and 13 show the distribution of boundary-correction factors, F_{ch}, along the crack front for two-symmetric quarter-elliptical corner cracks at a hole. The effects of crack size (a/t) on the distribution are shown in Figure 12. The finite-element results are shown as symbols and the proposed equation is shown as the solid curves. Again, the equation is in good agreement with the finite-element results, except near $\phi = 0$ and $\pi/2$. Here again the boundary-layer effect [19], as mentioned previously, is causing low values of boundary-correction factors. Further mesh refinement in this region was shown in the Appendix to give higher boundary-correction factors near the free surface, but lower values at the surface. Thus, the equation is expected to give a good estimate in these regions.

The effects of crack shape (a/c) on the distribution of boundary-correction factors are shown in Figure 13. Again, the proposed equation (solid curves) is in good agreement with the finite-element results (symbols), except near the intersection points ($\phi = 0$ and $\pi/2$).

In summary, for all combinations of parameters investigated and $a/t \leq 0.8$, the equations were within a few percent of the finite-element results. The maximum error was about 5 percent, except where the crack front intersects a free surface. For $a/t > 0.8$, the accuracy of the equations have not been established because there are no solutions available for comparison. However, their use in that range appears to be supported by estimates based on a part-through crack approaching a through crack. The effects of plate width on stress-intensity variations along the crack front were also included, but were

generally based on engineering estimates, Table 4 gives the range of applicability of ϕ, a/t, a/c, R/t, and (R + c)/b for the proposed equations.

CONCLUDING REMARKS

Stress-intensity factors from three-dimensional finite-element analyses were used to develop empirical stress-intensity factor equations for a wide variety of crack configurations subjected to remote uniform tension. The following configurations were included: an embedded elliptical crack, a semi-elliptical surface crack, a quarter-elliptical corner crack, a semi-elliptical surface crack at the center of a hole, and a quarter-elliptical corner crack at the edge of a hole in finite plates. The empirical equations cover a wide range of configuration parameters. The ratio of crack depth to plate thickness (a/t) ranged from 0 to 1, the ratio of crack depth to crack length (a/c) ranged 0.2 to 2, and the ratio of hole radius to plate thickness (R/t) ranged from 0.5 to 2. The effects of plate width (b) on stress-intensity variations along the crack front were also included, but were based on engineering estimates.

For all configurations for which ratios of crack depth to plate thickness do not exceed 0.8, the equations are generally within 5 percent of the finite-element results, except where the crack front intersects a free surface. Here the proposed equations give higher stress-intensity factors than the finite-element results, but these higher values probably represent the limiting behavior as the mesh is refined near the free surface. For ratios greater than 0.8, no solutions are available for direct comparison; however, the equations appear reasonable on the basis of engineering estimates.

The stress-intensity factor equations were also compared with other solutions reported in the literature for some of the configurations investigated. The proposed equations were in good agreement with some of the reported results. For limiting cases, as crack-depth-to-plate thickness (a/t) or crack-

depth-to-crack length (a/c) approach limits, the proposed equations reduce to exact or accepted solutions.

The stress-intensity factor equations presented herein should be useful for correlating and predicting fatigue-crack-growth rates as well as in computing fracture toughness and fracture loads for these types of crack configurations.

APPENDIX

Boundary-Layer Effect on Stress-Intensity Factors

Hartranft and Sih [19] proposed that the stress-intensity factors in a very thin "boundary layer" near the intersection of the crack with a free surface drop off rapidly and equal zero at the free surface. To investigate the boundary-layer effect, a semi-circular surface crack emanating from a hole was considered. Three different finite-element models were analyzed with 8, 10, and 14 wedges. A wedge is a slice of the finite-element model used to define a layer of elements [5]. The width of a wedge is measured by a parametric angle. Larger number of wedges result in smaller wedge angles and more degrees of freedom. The 8-wedge model had eight equal wedges ($\Delta\phi = \pi/16$). The other models had non-uniform wedges and were obtained by refining the 8-wedge model near the free surface ($\phi = \pi/2$). The smallest wedge angle for the 10- and 14-wedge models were $\pi/48$ and $\pi/180$, respectively. The stress-intensity factors obtained from the three models are shown in Figure 14. These results show that the stress intensities near the free surface were affected by mesh refinement. They were higher near the free surface but lower at the surface with smaller wedge angles. However, the stress-intensity distributions in the interior ($2\phi/\pi < 0.8$) were unaffected by mesh refinements.

Further mesh refinements near the free surface should give higher stress intensities near the free surface but lower values at the surface. Thus, the proposed equation (solid curve) is expected to give a good estimate for the limiting behavior due to mesh refinement.

REFERENCES

[1] Irwin, G. R.: The Crack Extension Force for a Part-Through Crack in a Plate, ASME, J. Appl. Mechs., Vol. 29, No. 4, 1962, pp. 651-654.

[2] Green, A. E.; and Sneddon, I. N.: The Distribution of Stress in the Neighborhood of a Flat Elliptical Crack in an Elastic Solid, Proc. Cambridge Phil. Soc., Vol. 47, 1950, pp. 159-164.

[3] Smith, F. W.; Emery, A. F.; and Kobayashi, A. S.: Stress Intensity Factors for Semi-Circular Cracks, Part 2 - Semi-Infinite Solid, J. Appl. Mechs., Vol. 34, No. 4, Trans. ASME, Vol. 89, Series E, Dec. 1967, pp. 953-959.

[4] Kobayashi, A. S.: Crack-Opening Displacement in a Surface Flawed Plate Subjected to Tension or Plate Bending, Proc. Second Int. Conf. on Mechanical Behavior of Materials, ASM, 1976, pp. 1073-1077.

[5] Raju, I. S.; and Newman, J. C., Jr.: Stress-Intensity Factors for a Wide Range of Semi-Elliptical Surface Cracks in Finite-Thickness Plates, Engineering Fracture Mechanics J., Vol. 11, No. 4, 1979, pp. 817-829. (See also NASA TM X-72825, Aug. 1977).

[6] Newman, J. C., Jr.; and Raju, I. S.: Analyses of Surface Cracks in Finite Plates Under Tension or Bending Loads, NASA TP-1578, Dec. 1979.

[7] Heliot, J.; Labbens, R.; and Pellissier-Tanon, A.: Benchmark Problem No. 1 - Semi-Elliptical Surface Crack, Int. J. of Fracture, Vol. 15, No. 6, Dec. 1979, pp. R197-R202.

[8] Tracey, D. M.: 3D Elastic Singularity Element for Evaluation of K Along an Arbitrary Crack Front, Int. J. of Fracture, Vol. 9, 1973, pp. 340-343.

[9] Pickard, A. C.: Stress Intensity Factors for Cracks with Circular and Elliptic Crack Fronts-Determined by 3D Finite Element Methods, PNR-90035, Rolls-Royce Limited, May 1980.

[10] Kobayashi, A. S.; and Enetanya, A. N.: Stress Intensity Factor of a Corner Crack, Mechanics of Crack Growth, ASTM STP-590, American Society for Testing and Materials, 1976, pp. 477-495.

[11] Shah, R. C.: Stress Intensity Factors for Through and Part-Through Cracks Originating at Fastener Holes, Mechanics of Crack Growth, ASTM STP-590, American Society for Testing and Materials, 1976, pp. 429-459.

[12] Smith, F. W.; and Kullgren, T. E.: Theoretical and Experimental Analysis of Surface Cracks Emanating from Fastener Holes, AFFDL-TR-76-104, Air Force Flight Dynamics Laboratory, Feb. 1977.

[13] Heckmer, J. L.; and Bloom, J. M.: Determination of Stress Intensity Factors for the Corner-Cracked Hole Using the Isoparametric Singularity Element, Int. J. of Fracture, Oct. 1977.

[14] Raju, I. S.; and Newman, J. C., Jr.: Stress-Intensity Factors for Two Symmetric Corner Cracks, Fracture Mechanics, ASTM STP-677, C. W. Smith, Ed., American Society of Testing and Materials, 1979, pp. 411-430.

[15] Raju, I. S.; and Newman, J. C., Jr.: Three-Dimensional Finite-Element Analysis of Finite-Thickness Fracture Specimens, NASA TN D-8414, May 1977.

[16] Tada, H.; Paris, P. C.; and Irwin, G. R.: The Stress Analysis of Cracks Handbook, Del Research Corporation, 1973.

[17] Gross, B.; and Srawley, J. E.: Stress-Intensity Factors for Single-Edge-Notch Specimens in Bending or Combined Bending and Tension by Boundary Collocation of a Stress Function, NASA TN D-2603, 1965.

[18] Newman, J. C., Jr.; and Raju, I. S.: An Empirical Stress-Intensity Factor Equation for the Surface Crack, Engineering Fracture Mechanics Journal, 1981.

[19] Hartranft, R. J.; and Sih, G. C.: An Approximate Three-Dimensional Theory of Plates with Application to Crack Problems, International Journal of Engineering Science, Vol. 8, No. 8, 1970, pp. 711-729.

[20] Howland, R. C. J.: On the Stresses in the Neighbourhood of a Circular Hole in a Strip Under Tension, Philos. Trans. R. Soc. London, Series A, Vol. 229, Jan. 1930, pp.49-86.

TABLE 1--Boundary correction factors, F, for embedded elliptical crack in a plate subjected to tension.

($c/b \leq 0.2$; $h/b = 1$; $\nu = 0.3$)

		a/t		
a/c	$2\phi/\pi$	0.2	0.5	0.8
	0	0.450	0.473	0.514
	0.125	0.531	0.556	0.605
	0.25	0.643	0.678	0.745
	0.375	0.750	0.794	0.884
0.2	0.5	0.838	0.893	1.015
	0.625	0.905	0.978	1.176
	0.75	0.951	1.042	1.329
	0.875	0.978	1.083	1.438
	1.0	0.987	1.097	1.480
	0	0.632	0.660	0.721
	0.125	0.656	0.685	0.749
	0.25	0.715	0.748	0.821
	0.375	0.789	0.826	0.905
0.4	0.5	0.857	0.900	0.995
	0.625	0.914	0.964	1.105
	0.75	0.954	1.014	1.211
	0.875	0.978	1.046	1.285
	1.0	0.987	1.056	1.312
	0	0.986	1.009	1.060
	0.125	0.986	1.009	1.058
	0.25	0.986	1.008	1.050
	0.375	0.986	1.006	1.035
1.0	0.5	0.986	1.006	1.036
	0.625	0.986	1.008	1.059
	0.75	0.986	1.010	1.093
	0.875	0.986	1.012	1.114
	1.0	0.986	1.013	1.121
	0	0.709	0.713	0.720
	0.125	0.703	0.707	0.714
	0.25	0.686	0.690	0.697
	0.375	0.658	0.662	0.669
2.0	0.5	0.622	0.625	0.633
	0.625	0.579	0.582	0.592
	0.75	0.536	0.539	0.552
	0.875	0.503	0.506	0.522
	1.0	0.490	0.494	0.511

TABLE 2--Boundary correction factors, F, for corner crack in a plate subjected to tension.

($c/b \leq 0.2$; $h/b = 1$; $\nu = 0.3$)

a/c	$2\phi/\pi$	a/t = 0.2	a/t = 0.5	a/t = 0.8
0.2	0	0.555	0.761	1.288
	0.125	0.633	0.840	1.340
	0.25	0.753	0.988	1.522
	0.375	0.871	1.141	1.705
	0.5	0.973	1.277	1.850
	0.625	1.055	1.397	2.008
	0.75	1.115	1.495	2.118
	0.875	1.159	1.580	2.263
	1.0	1.156	1.610	2.450
0.4	0	0.791	0.990	1.397
	0.125	0.774	0.952	1.297
	0.25	0.824	0.997	1.310
	0.375	0.893	1.067	1.346
	0.5	0.964	1.140	1.384
	0.625	1.026	1.210	1.458
	0.75	1.075	1.273	1.528
	0.875	1.117	1.334	1.627
	1.0	1.132	1.365	1.788
1.0	0	1.162	1.275	1.487
	0.125	1.111	1.207	1.378
	0.25	1.079	1.160	1.290
	0.375	1.064	1.134	1.219
	0.5	1.059	1.121	1.180
	0.625	1.063	1.123	1.191
	0.75	1.078	1.140	1.231
	0.875	1.109	1.176	1.301
	1.0	1.159	1.233	1.416
2.0	0	0.800	0.826	0.862
	0.125	0.787	0.811	0.837
	0.25	0.756	0.776	0.793
	0.375	0.722	0.738	0.750
	0.5	0.683	0.697	0.704
	0.625	0.640	0.653	0.660
	0.75	0.600	0.612	0.624
	0.875	0.579	0.590	0.611
	1.0	0.586	0.597	0.625

TABLE 3--Boundary correction factors, F, for surface crack at center of hole in a plate subjected to tension.

$((R + c)/b \leq 0.2;\ h/b > 1.6;\ \nu = 0.3)$

(a) $R/t = 1$

a/c	$2\phi/\pi$	a/t		
		0.2	0.5	0.8
0.2	0	0.641	0.607	0.593
	0.125	0.692	0.662	0.643
	0.25	0.836	0.775	0.771
	0.375	1.011	0.905	0.919
	0.5	1.196	1.032	1.094
	0.625	1.405	1.178	1.293
	0.75	1.651	1.362	1.528
	0.833	1.905	1.583	1.765
	0.917	2.179	1.885	2.050
	0.958	2.288	2.121	2.336
	1.0	1.834	1.958	2.329
0.4	0	1.030	0.872	0.840
	0.125	1.076	0.912	0.872
	0.25	1.202	1.007	0.959
	0.375	1.376	1.131	1.074
	0.5	1.578	1.275	1.234
	0.625	1.804	1.452	1.426
	0.75	2.040	1.667	1.668
	0.833	2.238	1.891	1.914
	0.917	2.396	2.141	2.201
	0.958	2.376	2.255	2.411
	1.0	1.844	1.923	2.224
1.0	0	2.267	1.806	1.615
	0.125	2.276	1.818	1.619
	0.25	2.301	1.851	1.630
	0.375	2.343	1.905	1.646
	0.5	2.404	1.980	1.730
	0.625	2.481	2.079	1.852
	0.75	2.566	2.206	2.049
	0.833	2.620	2.321	2.250
	0.917	2.622	2.415	2.452
	0.958	2.468	2.370	2.512
	1.0	1.950	1.957	2.203
2.0	0	1.944	1.606	1.394
	0.125	1.931	1.600	1.389
	0.25	1.897	1.582	1.377
	0.375	1.840	1.553	1.357
	0.5	1.763	1.514	1.333
	0.625	1.669	1.468	1.313
	0.75	1.580	1.434	1.310
	0.833	1.498	1.404	1.313
	0.917	1.426	1.387	1.332
	0.958	1.313	1.321	1.294
	1.0	1.042	1.082	1.077

TABLE 3--Boundary correction factors, F, for surface crack at center of hole in a plate subjected to tension.

((R + c)/b ≤ 0.2; h/b > 1.6; = 0.3)

(b) R/t = 2

a/c	2φ/π	a/t = 0.2	a/t = 0.5	a/t = 0.8
0.2	0	0.800	0.680	0.634
	0.125	0.864	0.743	0.690
	0.25	1.046	0.877	0.832
	0.375	1.272	1.037	1.002
	0.5	1.508	1.206	1.213
	0.625	1.766	1.410	1.469
	0.75	2.041	1.662	1.787
	0.833	2.279	1.932	2.109
	0.917	2.474	2.238	2.463
	0.958	2.439	2.375	2.699
	1.0	1.791	1.947	2.380
0.4	0	1.290	1.058	0.972
	0.125	1.346	1.107	1.010
	0.25	1.498	1.227	1.118
	0.375	1.704	1.384	1.263
	0.5	1.932	1.568	1.470
	0.625	2.165	1.785	1.722
	0.75	2.378	2.026	2.031
	0.833	2.516	2.237	2.319
	0.917	2.564	2.418	2.595
	0.958	2.417	2.416	2.705
	1.0	1.776	1.894	2.258
1.0	0	2.620	2.188	1.990
	0.125	2.626	2.199	1.996
	0.25	2.642	2.232	2.009
	0.375	2.667	2.280	2.026
	0.5	2.700	2.341	2.121
	0.625	2.732	2.410	2.246
	0.75	2.753	2.483	2.437
	0.833	2.733	2.527	2.599
	0.917	2.643	2.521	2.716
	0.958	2.409	2.381	2.662
	1.0	1.862	1.888	2.192
2.0	0	2.136	1.922	1.712
	0.125	2.121	1.911	1.704
	0.25	2.075	1.879	1.681
	0.375	2.000	1.826	1.643
	0.5	1.899	1.756	1.594
	0.625	1.777	1.671	1.541
	0.75	1.659	1.593	1.499
	0.833	1.552	1.522	1.461
	0.917	1.456	1.463	1.434
	0.958	1.325	1.360	1.351
	1.0	1.041	1.088	1.089

TABLE 4--Range of applicability for stress-intensity factor equations.

Configuration	Equation	ϕ	a/t	a/c	R/t	(R + c)/b
Embedded Crack in Plate	(3)	$-\pi$ to π	(a)	0 to ∞	...	<0.5[b]
Surface Crack in Plate	(16)	0 to π	(a)	0 to 2	...	<0.5[b]
Corner Crack in Plate	(26)	0 to $\frac{\pi}{2}$	<1	0.2 to 2	...	<0.2[b]
Surface Crack at Hole[c]	(38)	$-\frac{\pi}{2}$ to $\frac{\pi}{2}$	<1	0.2 to 2	0.5 to 2	<0.5
Corner Crack at Hole[c]	(49)	0 to $\frac{\pi}{2}$	<1	0.2 to 2	0.5 to 1	<0.5

[a] $a/t < 1.25\ (a/c + 0.6)$.

[b] $R = 0$.

[c] One or two-symmetric cracks.

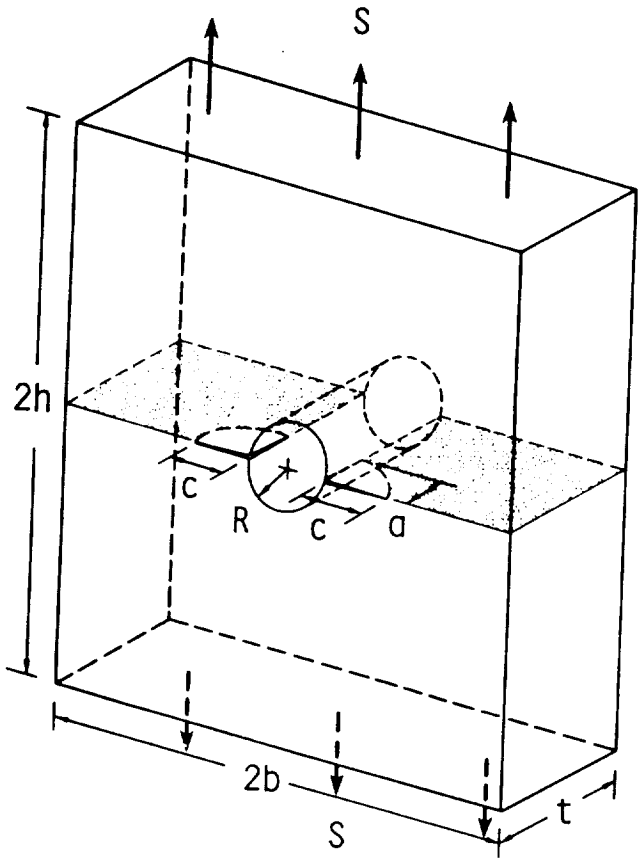

FIG. 1-Corner cracks at the edge of a hole in a finite plate subjected to remote tension.

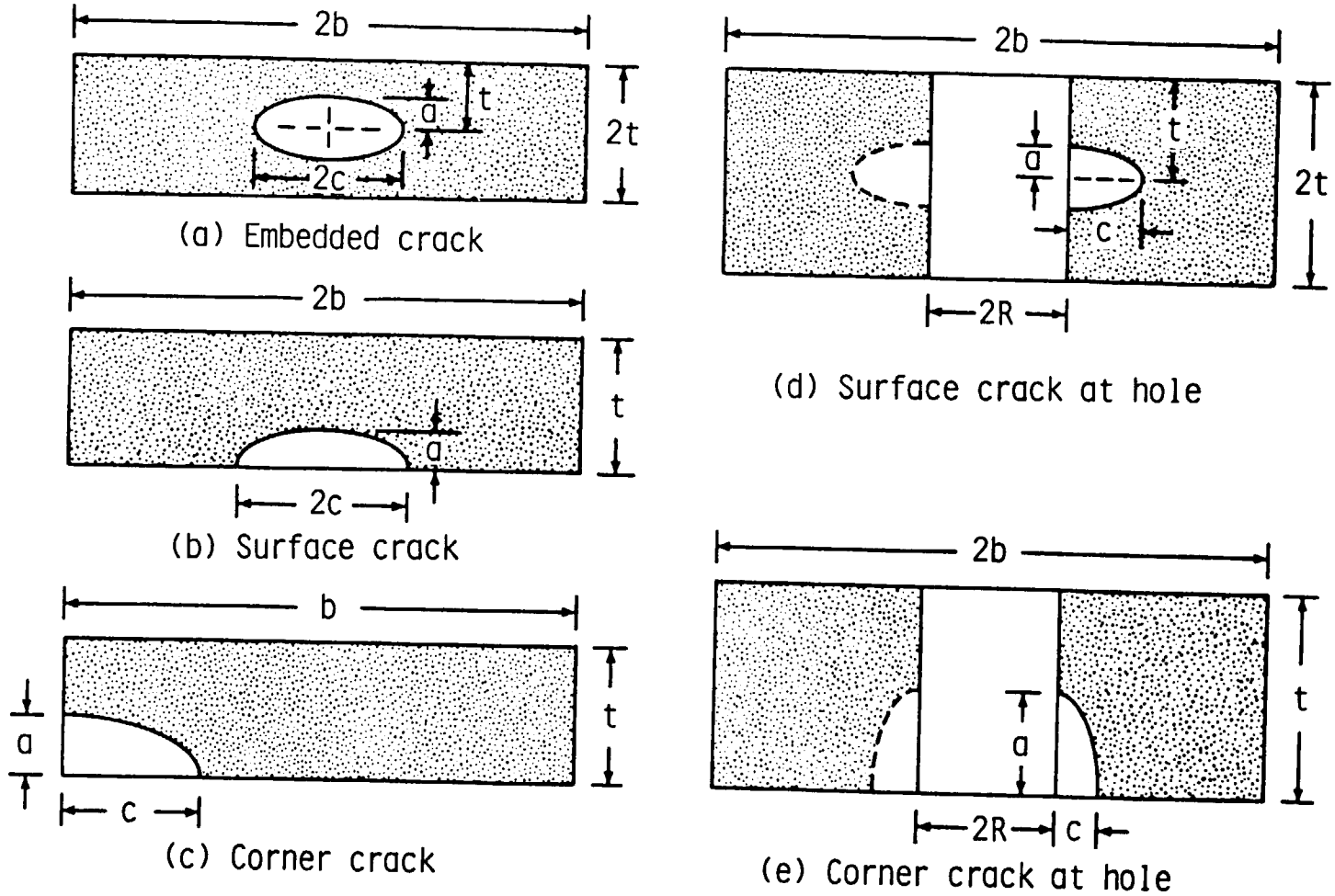

FIG. 2-Embedded-, surface-, and corner-crack configurations (all cracks have elliptical fronts).

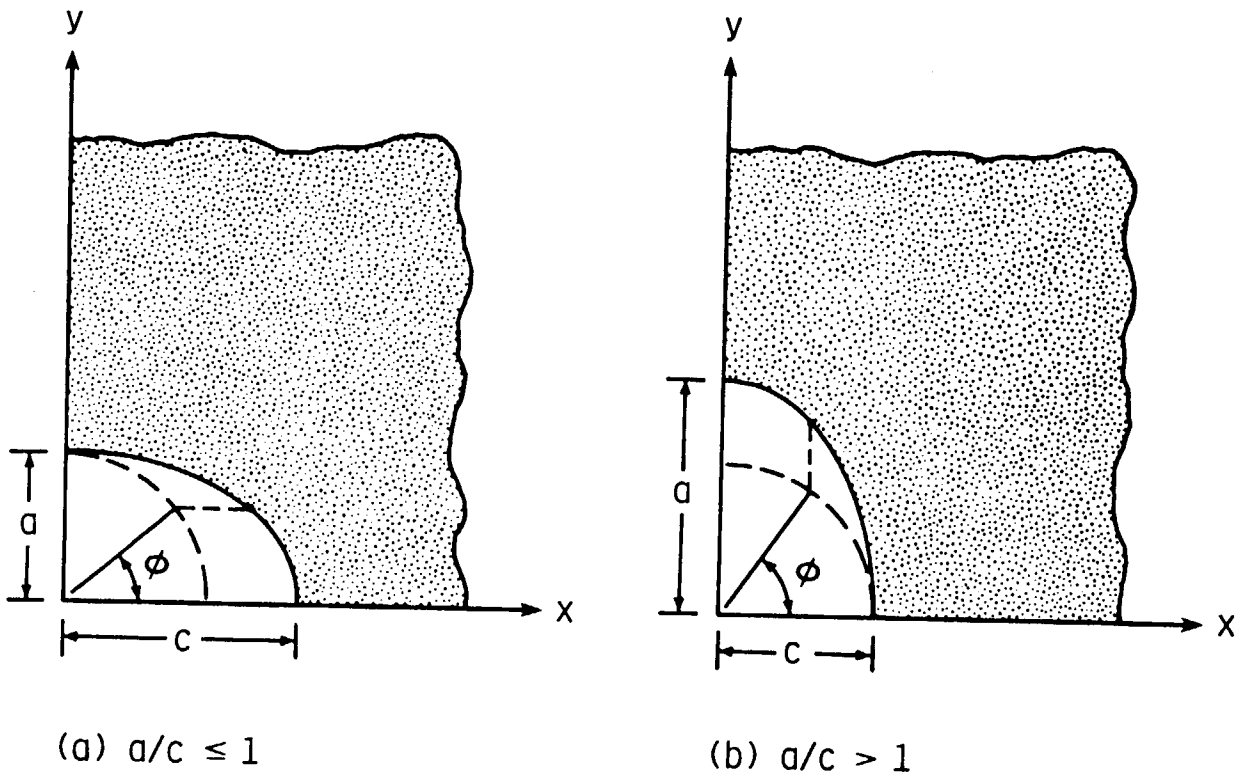

FIG. 3-Coordinate system used to define parametric angle.

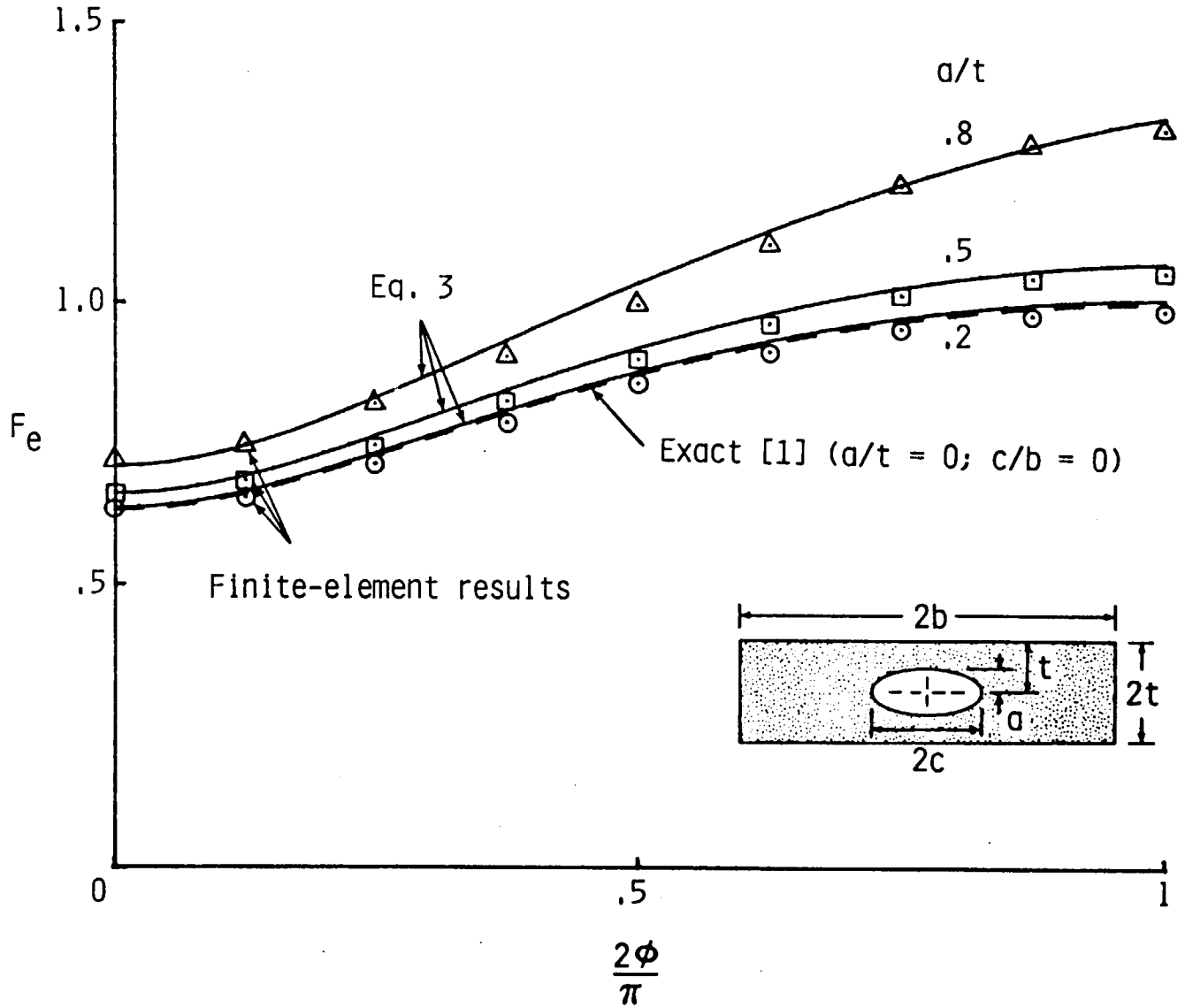

FIG. 4-Distribution of boundary-correction factors along crack front for an embedded elliptical crack (a/c = 0.4; c/b = 0.1).

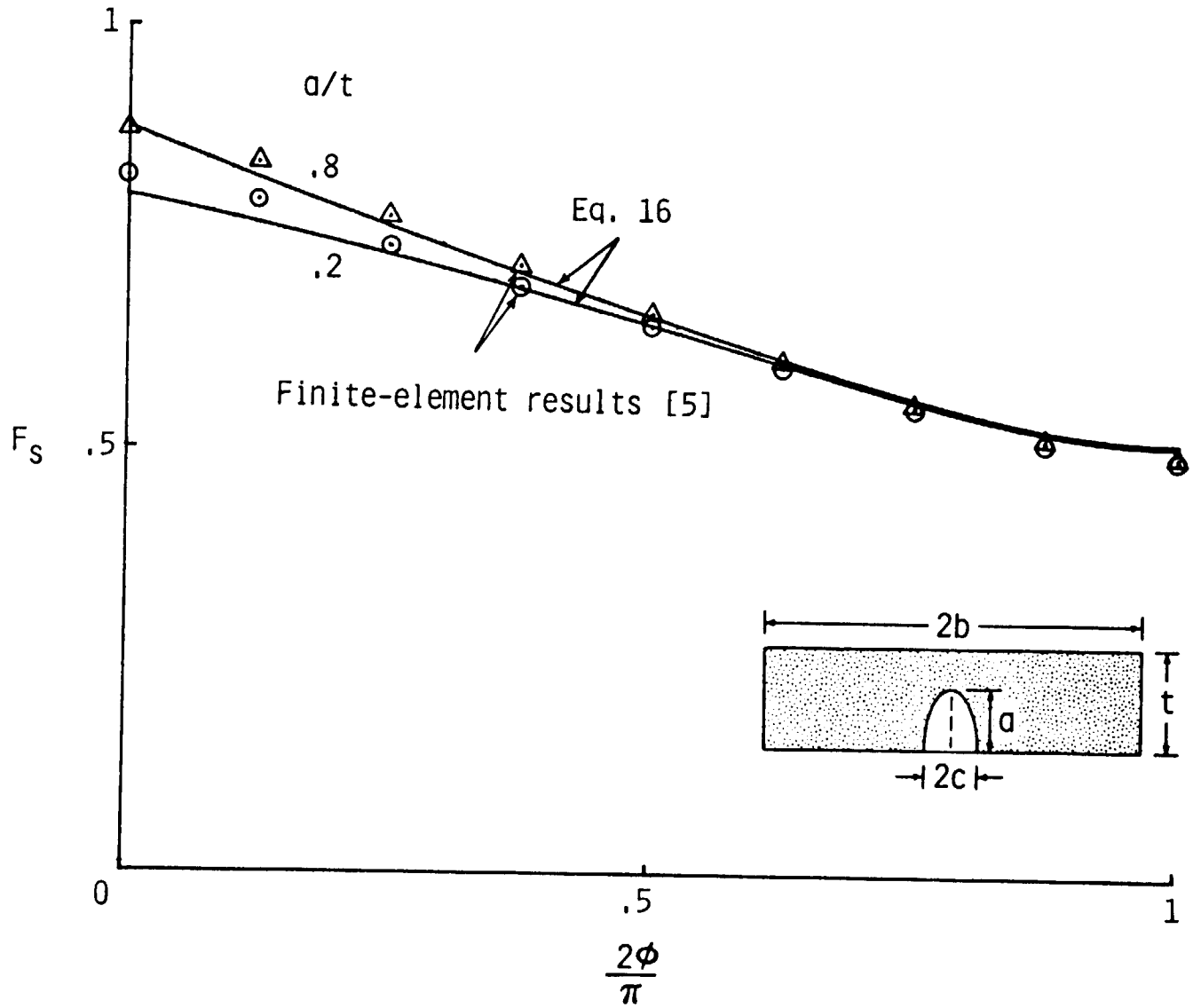

FIG. 5-Distribution of boundary-correction factors along crack front for a semi-elliptical surface crack (a/c = 2; c/b = 0.04).

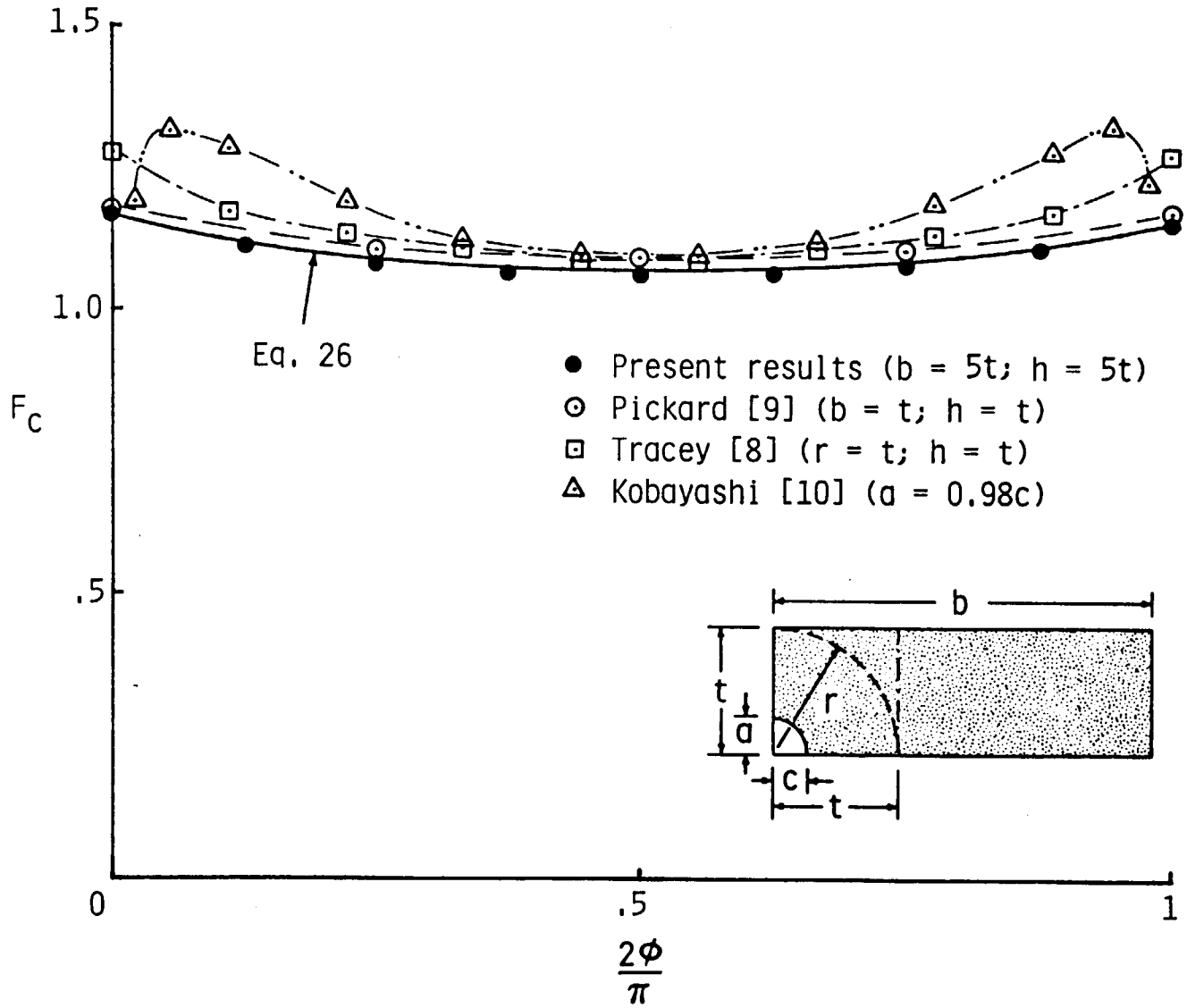

FIG. 6-Comparison of boundary-correction factors for quarter-circular corner crack in a plate subjected to tension (a/c = 1; a/t = 0.2).

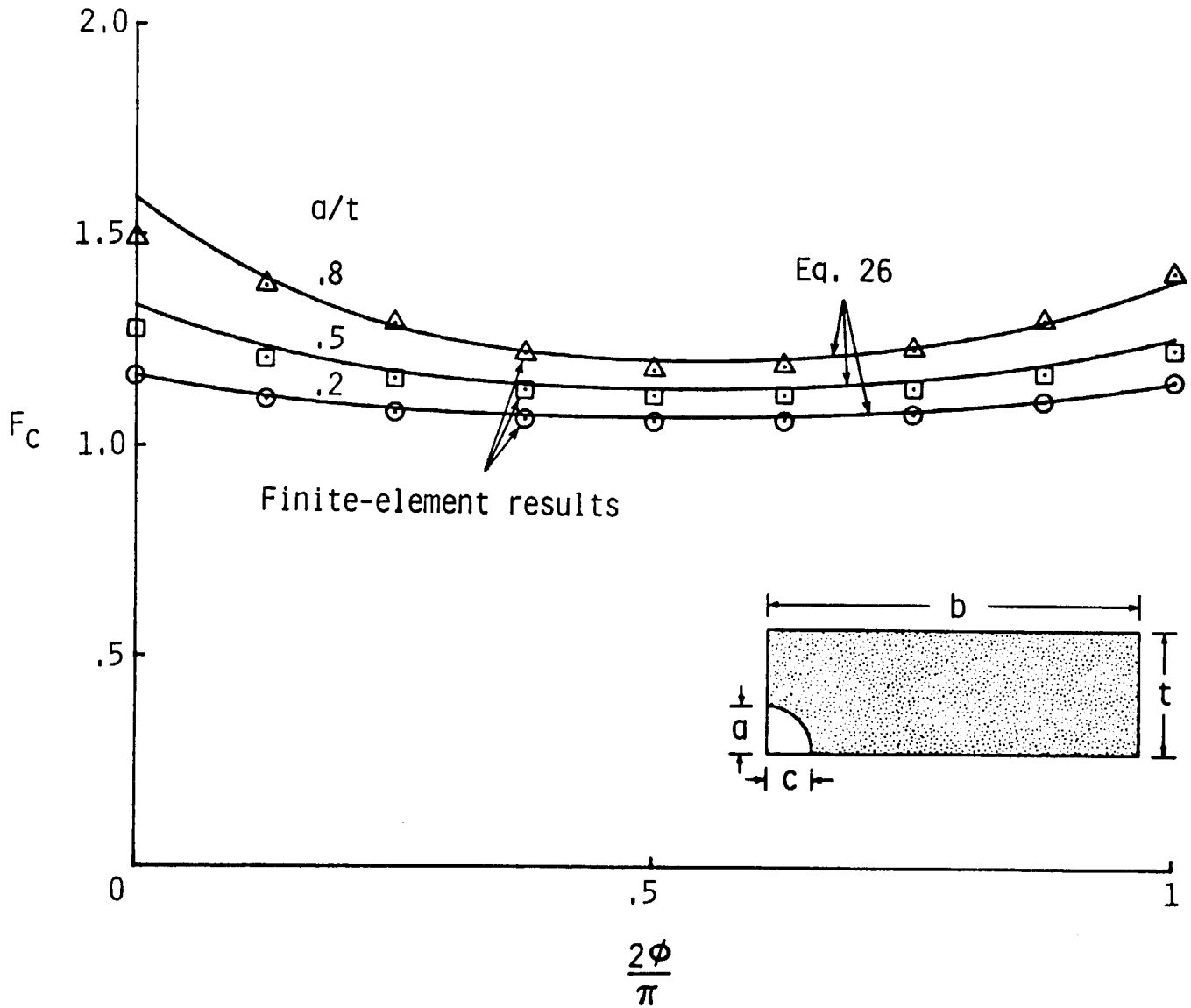

FIG. 7-Distribution of boundary-correction factors along crack front for quarter-circular corner crack (a/c = 1; c/b = 0.04).

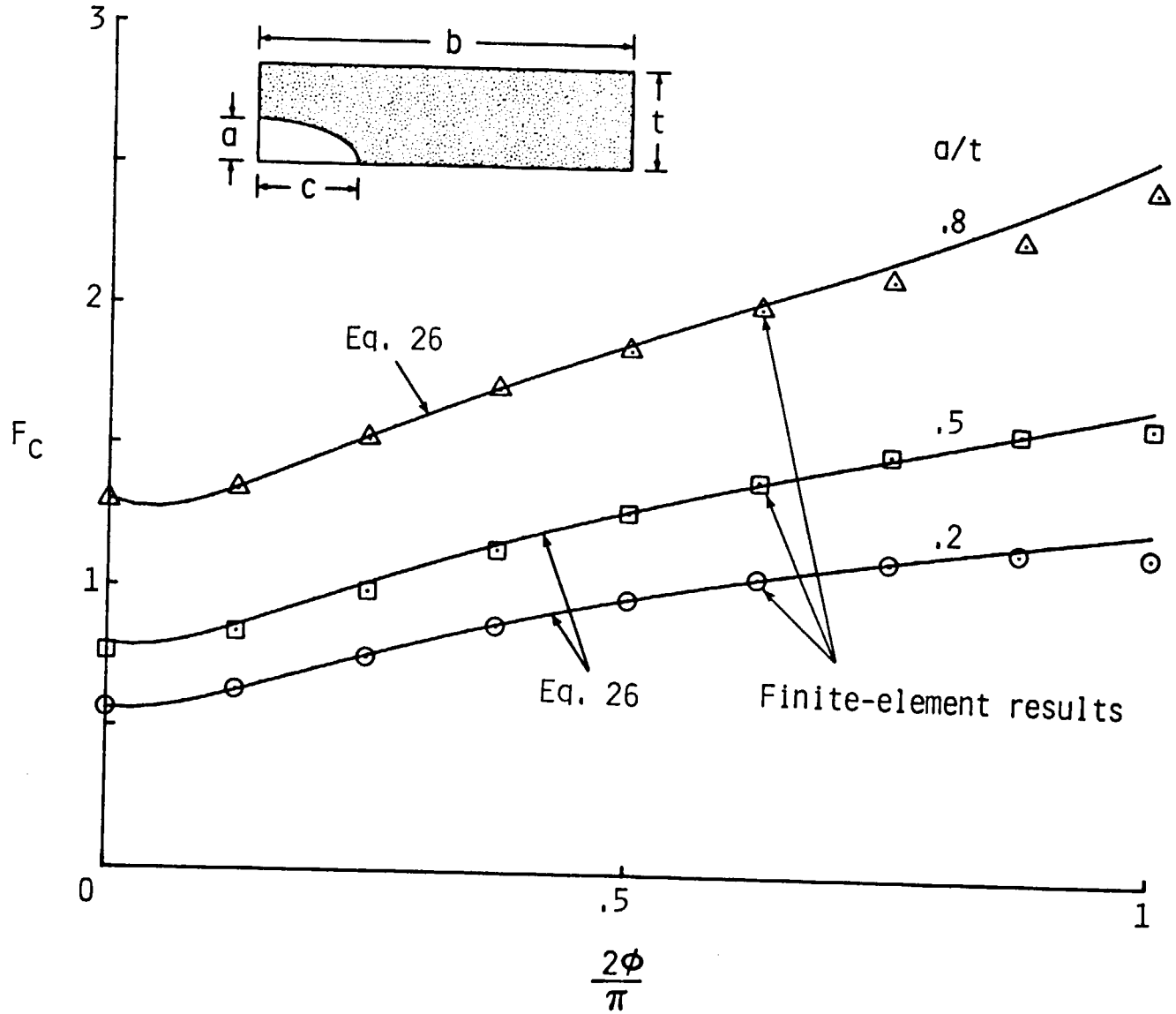

FIG. 8-Distribution of boundary-correction factors along crack front for quarter-elliptic corner crack (a/c = 0.2; c/b = 0.2).

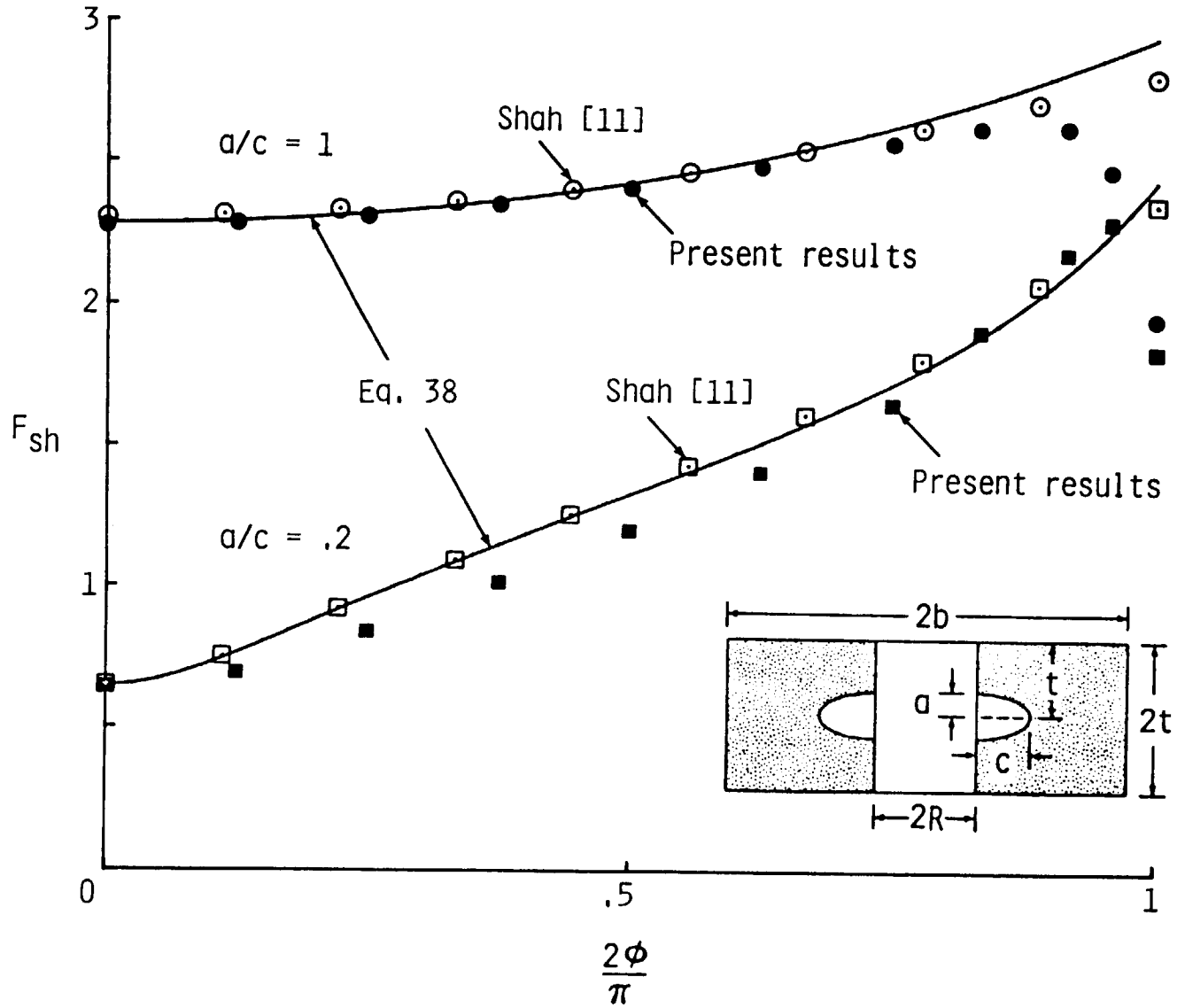

FIG. 9-Comparison of boundary-correction factors for semi-elliptical surface cracks at a hole subjected to tension (R/t = 1; a/t = 0.2; R/b < 0.05).

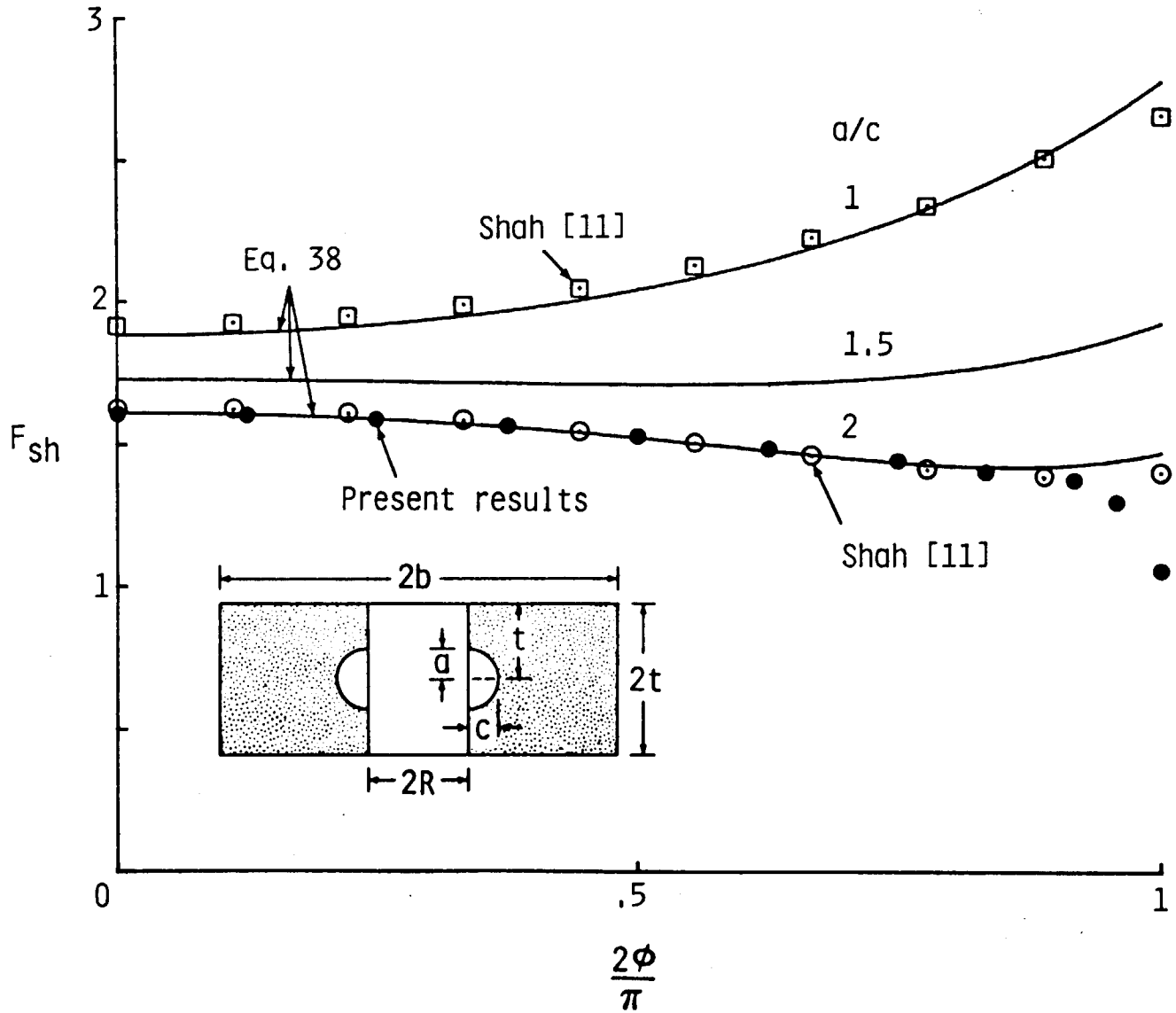

FIG. 10-Comparison of boundary-correction factors for semi-elliptical surface cracks at a hole subjected to tension as a function of a/c (R/t = 0.5; a/t = 0.2; R/b < 0.1).

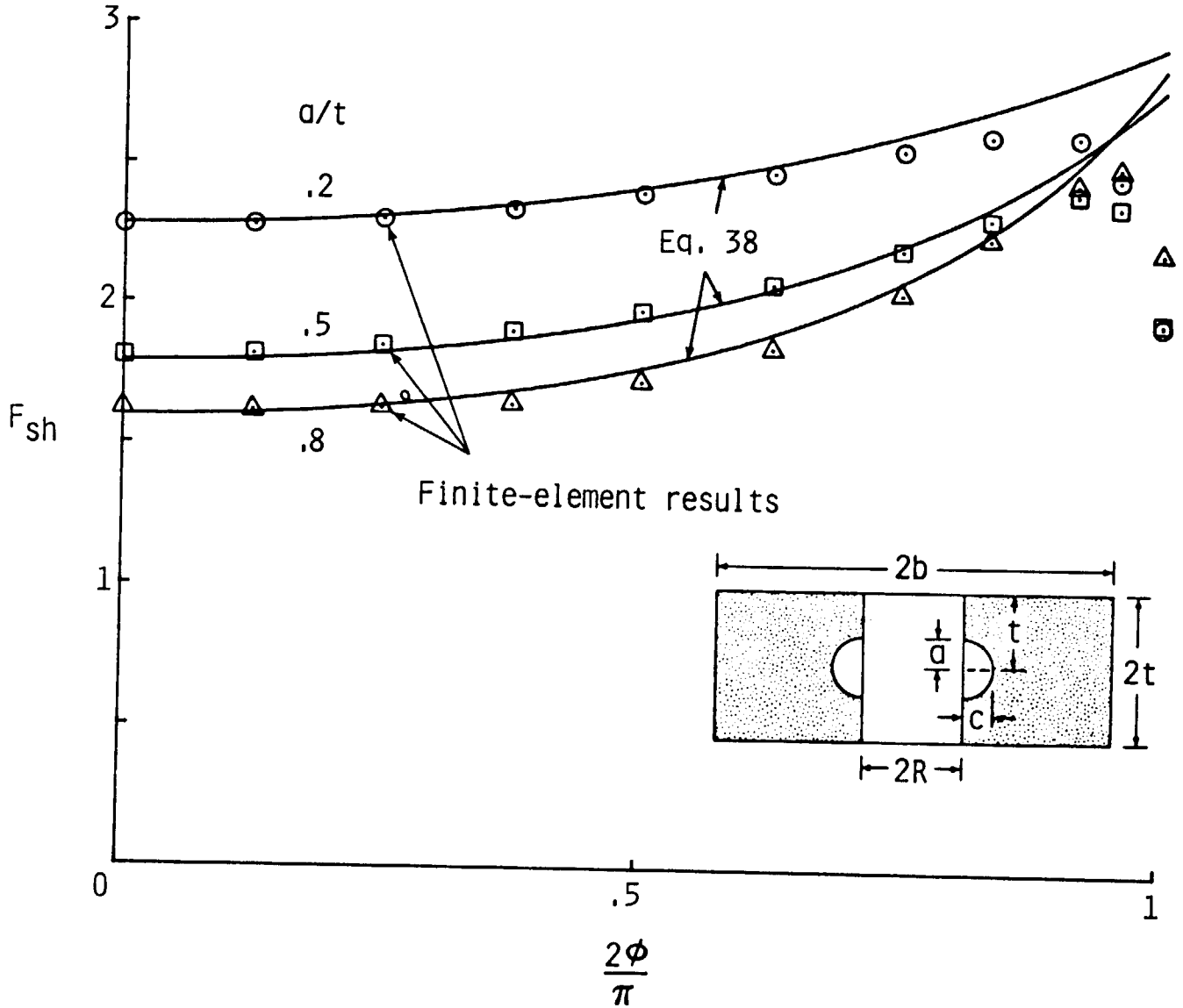

FIG. 11-Distribution of boundary-correction factors along crack front for semi-circular surface cracks at a hole (R/t = 1; a/c = 1; R/b < 0.1).

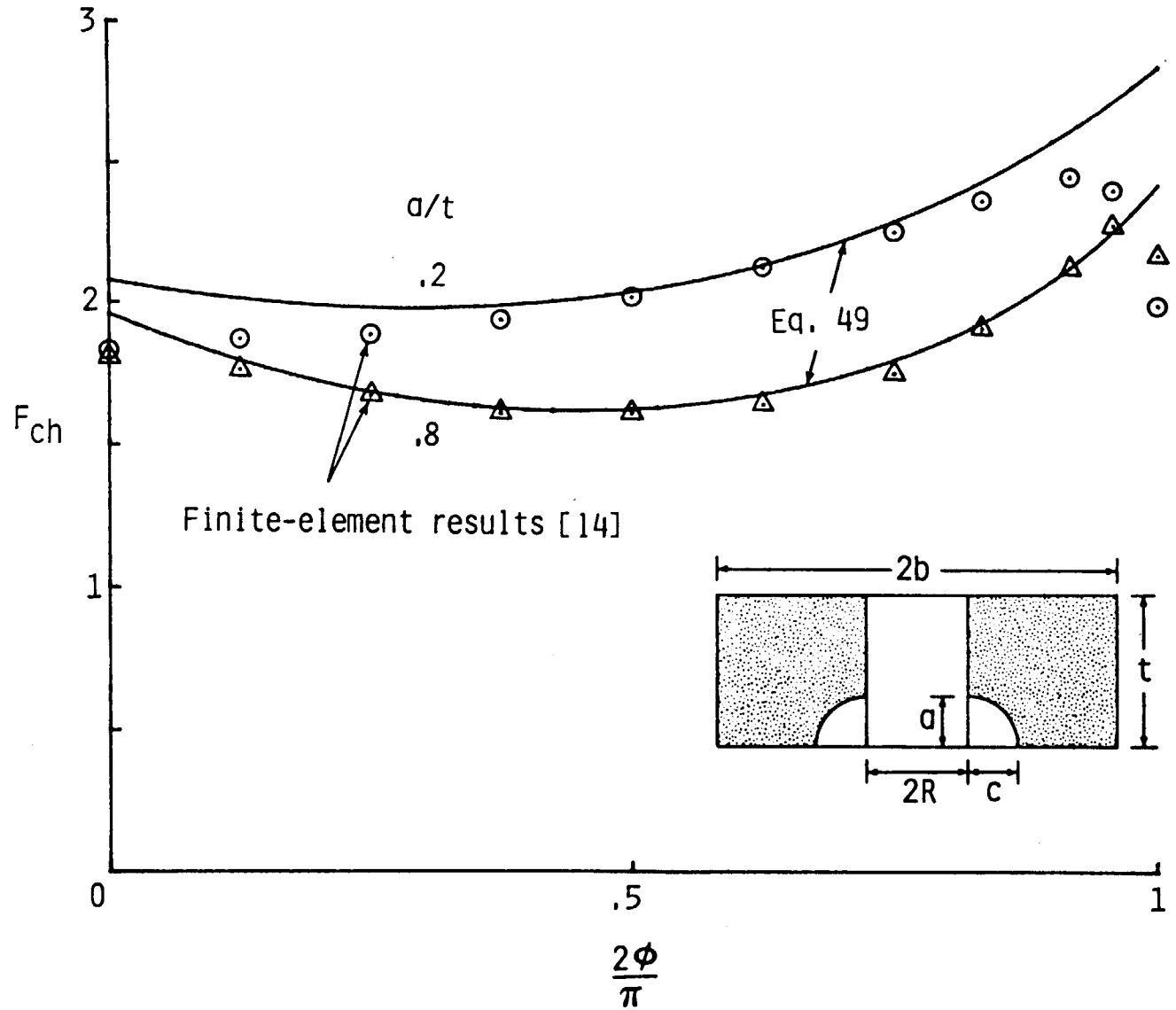

FIG. 12-Distribution of boundary-correction factors along crack front for quarter-circular corner cracks at a hole (R/t = 0.5; a/c = 1; R/b < 0.1).

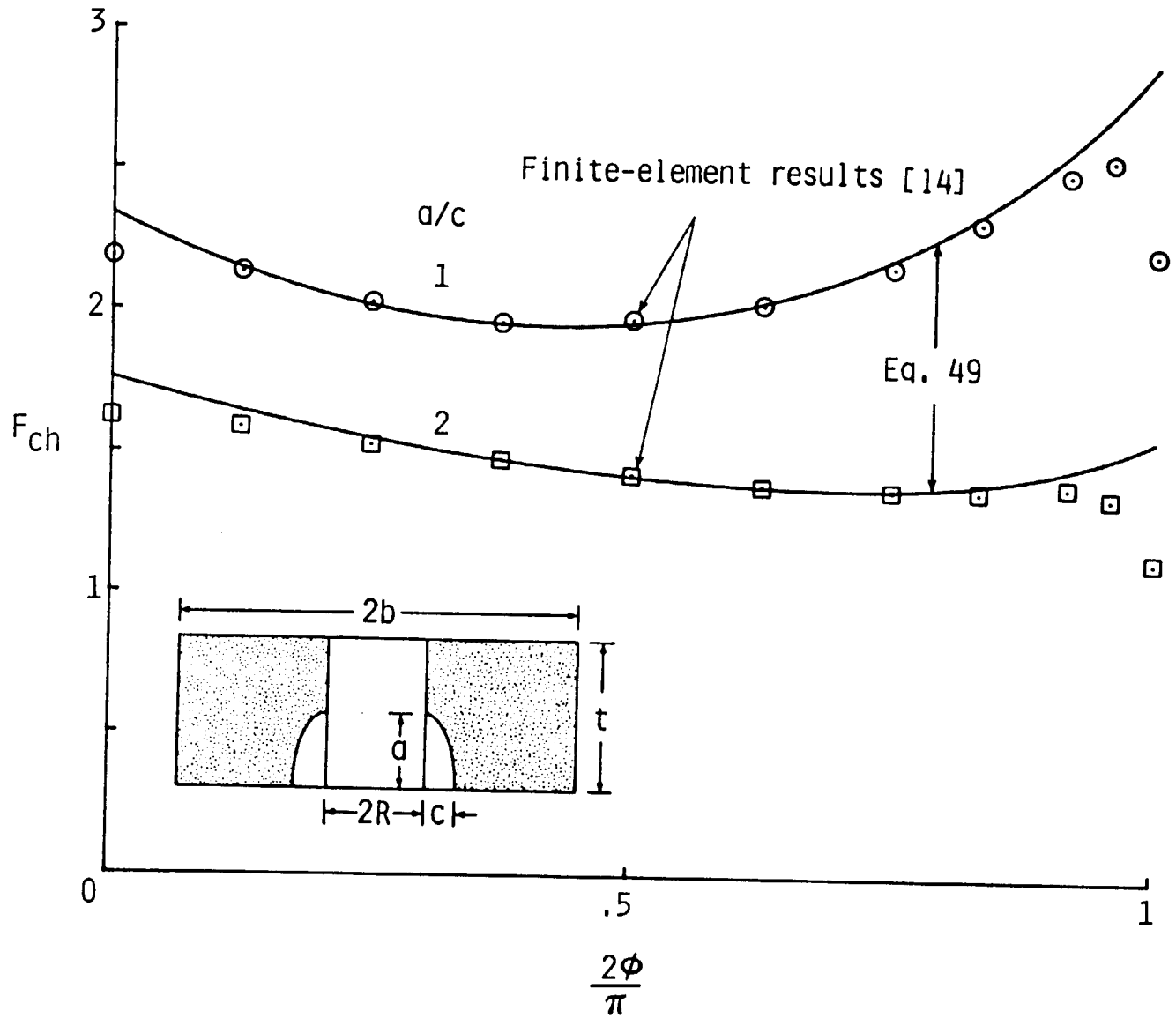

FIG. 13-Distribution of boundary-correction factors along crack front for quarter-elliptical corner cracks at a hole (R/t = 1; a/t = 0.8; R/b < 0.1).

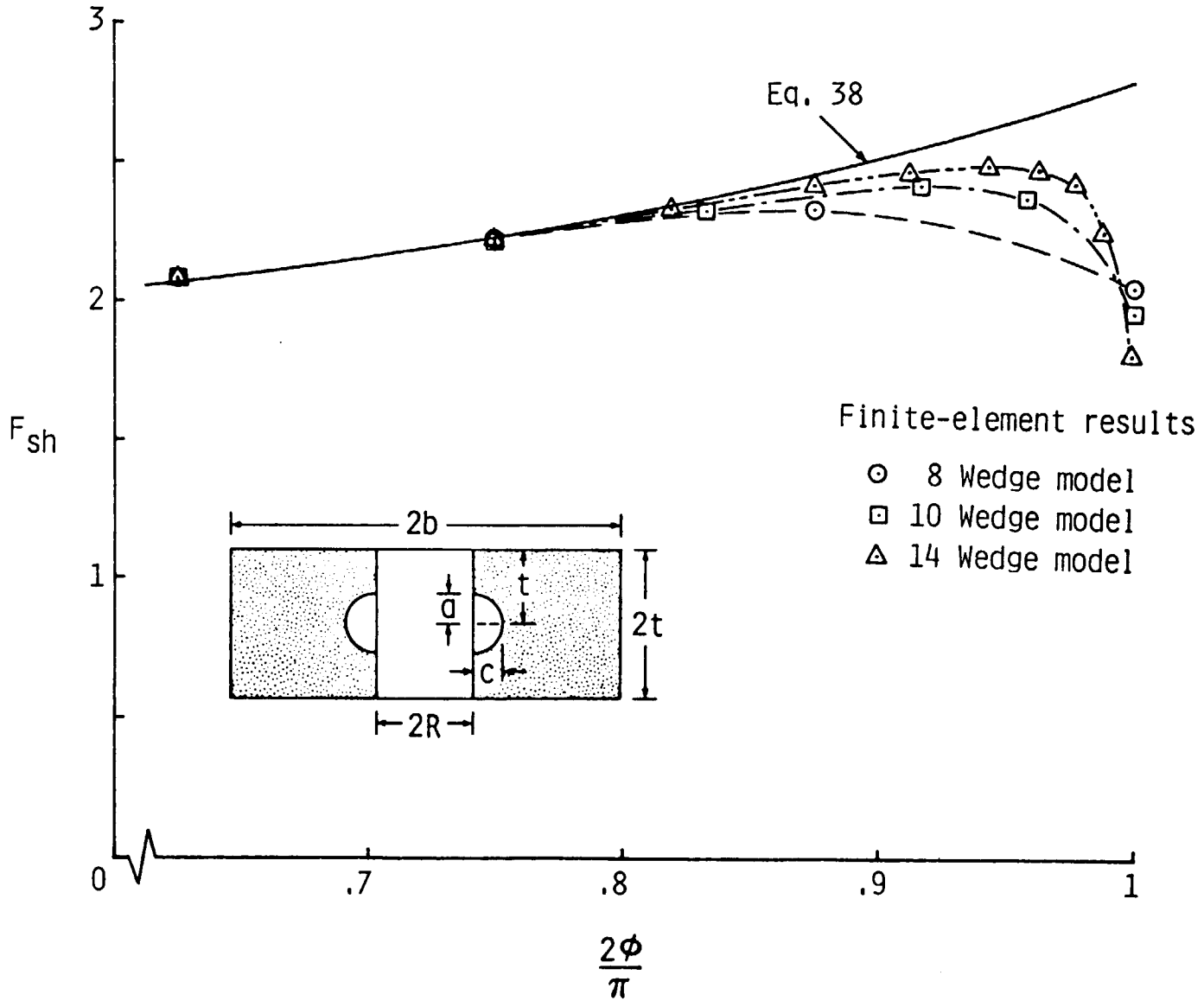

FIG. 14-Effects of mesh refinement near the free surface on the distribution of boundary-correction factors for surface cracks at a hole (R/t = 1; a/c = 1; a/t = 0.5; R/b < 0.05).

1. Report No.	2. Government Accession No.	3. Recipient's Catalog No.
NASA TM-83200		

4. Title and Subtitle	5. Report Date
STRESS-INTENSITY FACTOR EQUATIONS FOR CRACKS IN THREE-DIMENSIONAL FINITE BODIES	August 1981
	6. Performing Organization Code 505-33-23-02
7. Author(s) J. C. Newman, Jr. and I. S. Raju	8. Performing Organization Report No.
	10. Work Unit No.
9. Performing Organization Name and Address NASA Langley Research Center Hampton, VA 23665	11. Contract or Grant No.
	13. Type of Report and Period Covered Technical Memorandum
12. Sponsoring Agency Name and Address National Aeronautics and Space Administration Washington, DC 20546	14. Sponsoring Agency Code

15. Supplementary Notes

Presented at the ASTM 14th National Symposium on Fracture Mechanics, Los Angeles, California, June 30 - July 2, 1981.

16. Abstract

This paper presents empirical stress-intensity factor equations for embedded elliptical cracks, semi-elliptical surface cracks, quarter-elliptical corner cracks, semi-elliptical surface cracks at a hole, and quarter-elliptical corner cracks at a hole in finite plates. The plates were subjected to remote tensile loading. These equations give stress-intensity factors as a function of parametric angle, crack depth, crack length, plate thickness, and, where applicable, hole radius. The stress-intensity factors used to develop the equations were obtained from current and previous three-dimensional finite-element analyses of these crack configurations. A wide range of configuration parameters was included in the equations. The ratio of crack depth to plate thickness ranged from 0 to 1, the ratio of crack depth to crack length ranged from 0.2 to 2, and the ratio of hole radius to plate thickness ranged from 0.5 to 2. The effects of plate width on stress-intensity variations along the crack front were also included, but were generally based on engineering estimates. For all combinations of parameters investigated, the empirical equations were generally within 5 percent of the finite-element results, except within a thin "boundary layer" where the crack front intersects a free surface. However, the proposed equations are expected to give a good estimate in this region because of a study made on the boundary-layer effect.

These equations should be useful for correlating and predicting fatigue-crack-growth rates as well as in computing fracture toughness and fracture loads for these types of crack configurations.

17. Key Words (Suggested by Author(s))	18. Distribution Statement
Cracks Stress analysis Fatigue (materials) Fracture Stress-intensity factor Finite-element method	Unclassified - Unlimited Subject Category 39

19. Security Classif. (of this report)	20. Security Classif. (of this page)	21. No. of Pages	22. Price*
Unclassified	Unclassified	50	A03

* For sale by the National Technical Information Service, Springfield, Virginia 22161